AIAA SciTech Forum
23-27 January 2023, National Harbor, MD & Online
AIAA SCITECH 2023 Forum
10.2514/6.2023-1120

Electro-Optical Fiducial Markers on Satellites for Identification and Characterization

Novarah F. Kazmi Policht* and Teresa Nicole Brooks†
Ansys Government Initiatives, Exton, PA 19341, United States

Patrick North‡
Ansys Government Initiatives, Exton, PA 19341, United States

This paper demonstrates the benefits of applying electro-optical fiduciary markers on satellites for identification and characterization. Electro-optical fiduciary markers allow sensor systems, either on the ground or in space, to identify and characterize the target satellite with high accuracy and simple requirements. To evaluate the efficacy of this approach we trained a support vector machine (SVM) classifier on the synthetic imagery generated by Systems Tool Kit's (STK) Electro-Optical Infrared (EOIR) capability. We show how this novel approach and demonstrated workflow can be used to quickly identify and understand satellite targets of interest. Early results show positive identification of the target satellite, and the misidentifications can be attributed to the orientation of the satellite with respect to the sensor boresight.

I. Introduction

Our research explores the application of electro-optical fiduciary markers on satellites for the purposes of identification. As the number of satellites in orbit increases, there is a clear need to quickly identify them in a methodical way. A novel solution is to apply electro-optical fiduciary markers on the body of the satellite. Over an observational period the relative orientation changes over time, providing the observer with additional perspectives of the satellite. This should be understood to prevent misidentifying the target object.

A unique marker on a satellite would give it a distinct electro-optical signature, potentially allowing the observer to distinguish it from its counterparts in orbit, debris, or other Resident Space Objects (RSOs). Thus, minimizing or preventing misidentification. The key benefits include low cost, low risk, minimal weight, and no power requirement for added identification and characterization value. Additionally, these markers offer further unique identification and characterization opportunities with respect to spatial distribution patterns, spectral signatures, and active illumination of the markers. Another use case for this type of classification would be in the circumstances of rendezvous and proximity operations. The fiduciary markers can be utilized for alignment and docking, either as a servicing mission for life extension or for debris removal addressing the growing accumulation of space debris in critical orbital regimes [1]. Our ability to simulate the usage of electro-optical fiduciary markers to explore these ideas, highlights the important role that simulation software can play in the research space, as it allows us to easily and inexpensively explore ideas using high-fidelity simulated data in a risk-free environment.

To demonstrate the applicability and viability of this approach, we used Systems Tool Kit (STK) to simulate a scenario utilizing these markers and both ground and space based representative Space Situational Awareness (SSA) or Space Domain Awareness (SDA) sensors. Then we compared how the same SSA/SDA sensor systems were able to identify a target satellite with and without the electro-optical fiduciary markers. STK's Electro-Optical Infrared (EOIR) modeling capability "incorporates all necessary components for modeling sensor-based systems into a single program" [2]. STK modeled the orbit, attitude, 3D-model of the target satellite, the configuration of the electro-optical markers on the body of the satellite, as well as the SSA/SDA imaging sensor systems. The goal was to see if any markers on the body of the satellite could be positively identified by a support vector machine (SVM) [3], [4] classifier. For this study, the target satellite was in Low-Earth orbit and observed over a specified period where the satellite was illuminated by the Sun.

*Senior Application Engineer, Pre-Sales Support, 220 Valley Creek Blvd., Exton, PA 19341
†Principal R&D Engineer, Digital Mission Engineering, 220 Valley Creek Blvd., Exton, PA 19341
‡Principal R&D Engineer, Digital Mission Engineering, 220 Valley Creek Blvd., Exton, PA 19341

Using STK's EOIR modeling capability, we synthetically imaged the satellite during the specified interval to generate observations from both ground-based and space-based sensor systems. STK gives us the flexibility to modify the markers in each run of the scenario. The output files from STK EOIR are bitmap formatted image files and the corresponding raw sensor data of the pixels in electron counts as text files. The data was collected by two sensor systems, providing two views of the target satellite. By running the scenario to model the target satellite with and without the electro-optical markers, we generated two classes of data. The resulting data was used to train and evaluate a classifier model to identify electro-optical markers on the body of a target satellite.

Preliminary results show that we can accurately identify the target satellite with an electro-optical marker. The approach presented here can be replicated for satellites in different orbits and with different markers. This is due to STK's time-dynamic multi-domain environment and our usage of machine learning to build robust image classifiers. The workflow presented here will show the benefit of using fiduciary markers for quick identification and understanding of objects in orbit.

II. Related Work

With the growing presence of manmade objects in space, there is a need to positively identify them. Being able to quickly establish and understand nearby RSOs increases awareness and safety of all missions. We see in past works strategies utilizing synthetic data and Artificial Intelligence / Machine Learning (AI/ML) for addressing this challenge.

A. Simulated Sensor System Data for RSO Identification

One method for addressing this challenge is to generate simulated data of what a sensor system would see. McQuaid, demonstrated using Systems Tool Kit (STK) to generate datasets from modeled targets (geostationary satellites), assets, and payload sensor systems [5]. In this research, the sensors were modeled with unique spatial, spectral, optical and radiometric characteristics. The generated dataset was used to train deep neural network (DNN) that automatically associates observations with their corresponding Resident Space Objects (RSOs). The results were promising, where in future research they continue working with multiple channels or in different areas of the spectrum [5]. In our research we leverage similar workflows used by McQuaid and apply novel electro-optical fiduciary markers as unique characteristics of the target satellites.

B. Using Generated Imagery Datasets in Machine Learning

Additionally, researchers have used generated imagery datasets to train machine learning models for classification and object detection tasks. Fletcher, et al, trained convolution neural networks (CNN) [6], [7] to detect geosynchronous Earth orbit (GEO) RSOs on both collected imagery from electro-optical ground-based telescopes and synthetically generated datasets [8]. They were able to improve model sensitivity to "low-frequency occurrences" [8] by augmenting the naturally collected training data with synthetical generated data, which enabled them to increase the number of training examples for valid but less frequent scenarios. Despite the challenges in the "lack of diversity among naturally-collected data, and the absence of relevant phenomena in simulated data" [8] their detection model yielded impressive results. Other works have used spectroscopy, both simulated and real data in training convolution neural networks (CNNs) to identify satellites and note that resolved imagery would be ideal for characterization [9].

Prior research has demonstrated the promise of using simulated data with machine learning to identify RSOs. While there are features that a model can be trained on, we propose the placement of electro-optical fiduciary markers on the satellite. These markers create a unique phenomenon on the satellite and allow it to be differentiated from similar RSOs. While training machine learning models on real imagery is ideal, it requires a mission operator to have a system in place for observations. Also, using simulated data enables the user to increase both the volume and complexity of data as required by a specific learning task. These qualities of simulated data were especially useful for this study. The unique electro-optical fiduciary markers data do not exist, so we relied on generated sensor imagery. We leverage the STK EOIR capability to generate our synthetic sensor data.

C. Support Vector Machines

In the world of machine learning there are no shortages of classifier models to choose from. While deep neural networks (DNNs) are very popular for many learning tasks including image classification and object detection, they require very large amounts of data and an enormous amount of computing power. For classification tasks where the number of features is very large relative to the size of the training data, support vector machines (SVMs) are a promising alternative to DNNs for image classification and detection tasks in various domains [10], [11], [12], [13].

SVMs are a “vector-based” [14] machine learning model. They seek to maximally separate two classes via a learned decision boundary. They were first introduced by Vapnik [4] and have yielded state of the art results in various problem spaces from pattern recognition to text classification for decades. Though they are not without their limitations, SVMs models are very flexible models that can be used for both classification and regression tasks and via the use of kernel functions they can be used to build classifiers for both linearly and non-linearly separable data. SMVs also offer relatively easy to interpret results.

The primary objective of this preliminary research was to determine if we could identify a satellite that had an electro-optical fiduciary marker. With this objective in mind, we limited our model selection to a small subset of machine learning models, as we wanted easy to train, interruptible binary classifier models. SVMs were chosen for this task as they yield flexible and interruptible models.

III. Materials and Methods

The exploration of unique electro-optical fiduciary markers in conjunction with machine learning begins with simulation. It is initiated by simulating the target satellite with and without the spectral markers. These markers peak at a specified wavelength corresponding with our modeled sensors. Our study proposes using these markers, STK EOIR’s data generation capability, along with machine learning as a possible workflow to address the challenges of RSO classification for Space Situational Awareness/Space Domain Awareness (SSA/SDA).

A. Systems Tool Kit (STK)

Using STK, we modeled a scenario with a target satellite coming into view over a ground site. Simultaneously, a second satellite in Low Earth Orbit (LEO) also views the target satellite. Both the ground site and the observing LEO satellite are equipped with hypothetical SSA/SDA sensors. Both capture images of the target satellite when it is in view using STK v12.4 EOIR capability [15].

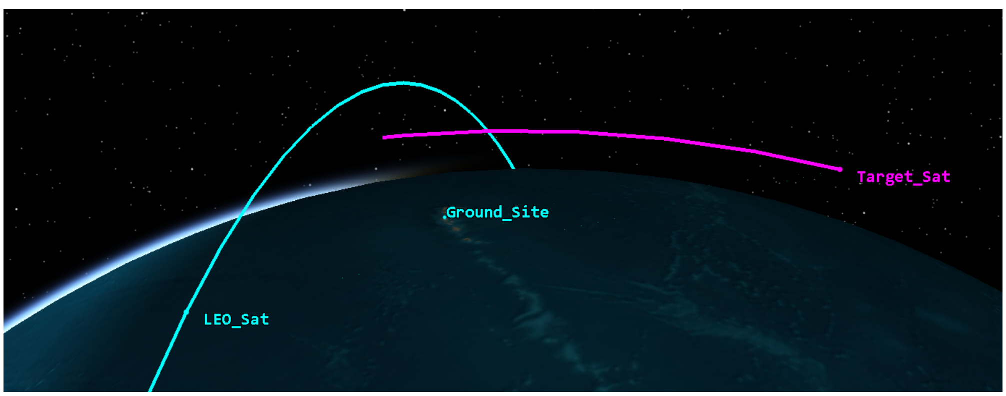

Fig. 1 View of the STK scenario, the target satellite and its trajectory is indicated in fuchsia, the observing satellite and ground site are in teal.

Each sensor detects in the 0.70-5.0 µm region of the electromagnetic radiation spectrum. The sensor settings were configured to give us a resolved image of the target. The spatial, optical, and radiometric settings were optimized for visual detection. These notional sensor parameters were selected with the goal of bringing the image of the target satellite into view. Non-specified parameters were left with their default values.

The target satellite was simulated to orbit in LEO and in close proximity to the nearby observing systems. Its attitude was set to nadir alignment with ECI velocity constraint, which kept the satellite at the same orientation for the entire imaging duration. Due to the satellite’s orientation, the scenario time, and the position of the two observing sensors, the satellite is illuminated by the Sun and its material characteristics are reflected and captured by both sensors. A custom but simple CubeSat 3D model was used. A single face of the main CubeSat body was divided into a 4 by 4 grid, creating 16 sections. This is the primary panel. By having sections, we could define custom material and spectral characteristics of a component of the model.

To model the electro-optical fiduciary markers, we created a custom spectral reflectance file (SRF) that peaked

Table 1 EOIR Sensor Parameters

Sensor Parameter Name	Value
Horizontal & Vertical Half Angle	0.0005 deg
Horizontal & Vertical Number of Pixels	250 px
Spectral Band Edge Wavelengths	0.7 - 5.0 µm
F/#	2.0
Effective Focal Length	110 m
Sensitivity – Equivalent Value	1e-19 Wcm^{-2}

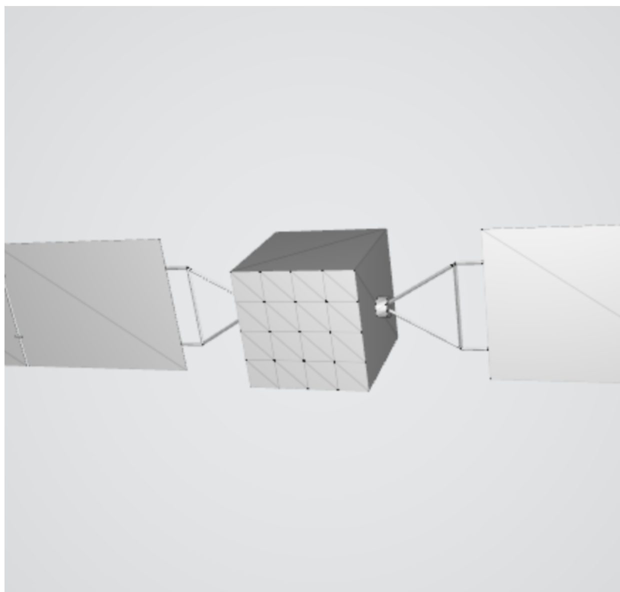

Fig. 2 Simple 3D model of CubeSat with the primary panel divided into sections.

Table 2 EOIR 3D Model Properties

EOIR Shape Parameters	Value
Electro-Optical Fiduciary Markers	Custom Spectral reflectance file 0.7 - 5 µm
Bus exterior	Gold MLI
Rods	Gray Body - 50 % reflectance
Solar Panels	Solar Panels

between 0.7 - 5.0 µm. This reflectance file was used to model the reflectance characteristics of 5 out of the 16 panels, the rest of the bus exterior being modeled with Gold MLI [16]. The markers were placed in a distinct pattern to differentiate it from the general satellite. Only one side of the satellite had the markers, the side that would face the Sun and be in view of the observing ground site and neighboring satellite.

STK is a time dynamic tool, and we leveraged this aspect of it to animate over a specified duration in which the target satellite was in view and illuminated by the Sun. We ran the scenario simulation a few times. Having to run the scenario for each configuration of the primary panel, with and without markers. Later, we extended the imaging duration and again generated data for each configuration of the primary panel. We were able to capture images from both the ground and space-based sensors simultaneously.

Initially, the imaging interval was shorter, we generated 120 frames for each sensor over a 2-minute scenario time, and with each primary panel configuration. In total we generated 480 frames. For the later run, we extended the

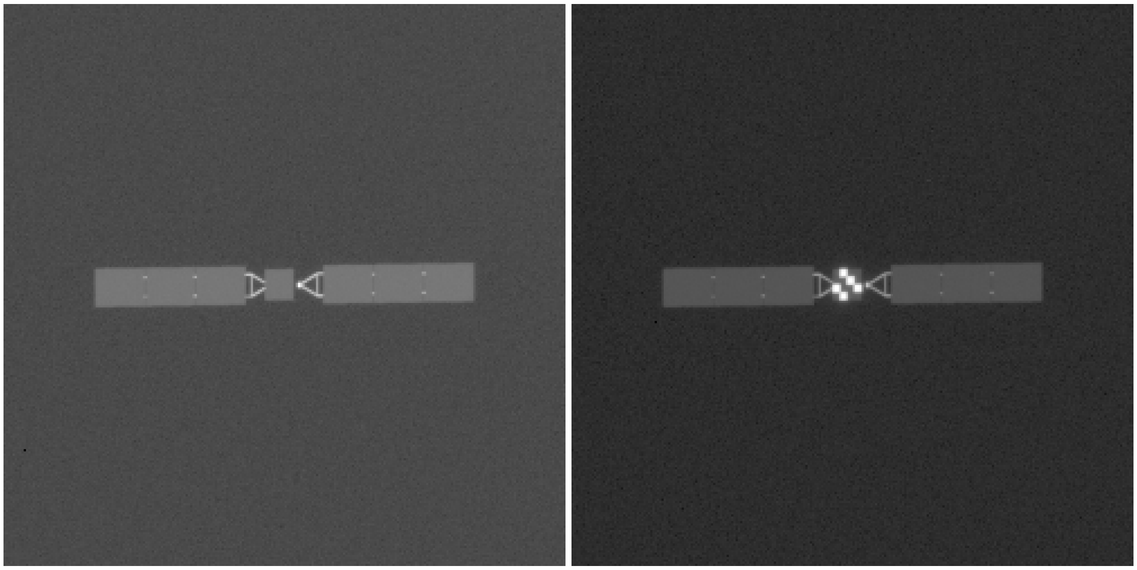

Fig. 3 Satellite's sensor synthetic image of the target satellite without and with electro-optical fiduciary markers.

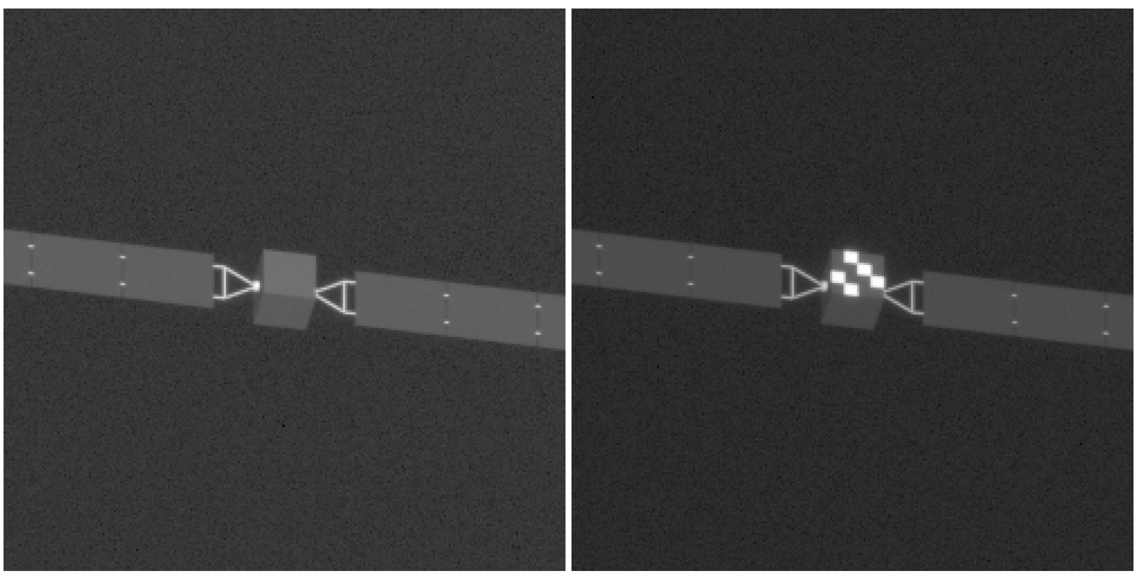

Fig. 4 Ground site's sensor synthetic image of the target satellite without and with electro-optical fiduciary markers.

observation period, allowing the satellite to come into view from a further distance. This was a 5 min and 16 second scenario time. We generated 1,580 frames per configuration per sensor for each model of the primary panel. From this run we generated a total of 6,320 frames.

The data was exported as bitmap files and text files of the raw sensor data of the pixels in electron counts. We were able to repeat the experiment, changing the duration, the presence of the fiducial markers, and exporting the results, without having to rebuild the scenario.

The examples in Fig. 3 and Fig. 4 show images of the target satellite by the two sensors at different times to demonstrate the changing relative collection orientation. From the viewpoint of the observing satellite, it sees the target satellite's primary panel for most of the scenario. From the ground site, and with the understanding that the sensor is viewing the scene from below, we see the primary panel but also the underside of the target satellite. The raw data from the ground site sensor had no pre-defined "up" direction, and the images have been rotated for clarity.

B. Dataset Design

We modeled this problem as a computer vision, image classification problem as this made it easier to test our ability to identify a satellite with an electro-optical fiduciary marker. It also made model performance interpretation and example misclassification analysis easier. Table 3 lists a summary of size and duration characteristics of all generated datasets used to train and evaluate our binary classifier models that identify a satellite with an electro-optical fiduciary marker. Note, the positive class examples are the satellites with the electro-optical fiduciary marker and the negative class examples are the same satellites without the marker.

Table 3 Summary of size and duration characteristics of generated datasets.

Dataset	Duration	# Of Frames	# Of Positive Class Examples	# Of Negative Class Examples
Ground Sensor (Short Duration)	2 min	120	120	120
Satellite Sensor (Short Duration)	2 min	120	120	120
Ground Sensor (Long Duration)	5 min 16 sec	1580	1580	1580
Satellite Sensor (Long Duration)	5 min 16 sec	1580	1580	1580

Our primary objective of this preliminary research was to determine if we could identify a satellite that had an electro-optical fiduciary marker. Given this objective we made a deliberate effort to model the problem as simply as possible with the understanding that future research efforts would focus on more complex and nuanced versions of this problem. The datasets generated for this research directly reflect our objectives.

With our objectives in all generated datasets have the following criteria:

1) Balanced Datasets: Each dataset must have the same number of positive and negative classes. This ensured that we avoided typical issues when working with and training classifier models on imbalanced datasets.
2) Single Attitude for All Examples: An altitude profile of nadir alignment with ECI velocity constraint kept the satellite at the same orientation for the entire imaging duration. This reduced the perspective changes; the satellite does not rotate, and the primary panel remains in sunlight. By simplifying the orientation, we see in the dataset that the change in perspective is due to the angle and distance to and from the observer as the target satellite travels in its orbit, not because the satellite itself is rotating in space.
3) All Positive Class Satellites Have The Same Electro-Optical Marker: Our preliminary research models the marker identification problem as a binary classification problem, meaning we only want to determine if the satellite has the electro-optical fiduciary marker, or it doesn't. This means that in each positive class example the satellite must have the same marker across all four datasets.
4) All Positive and Negative Class Examples Must Contain The Same Satellite: In each dataset all negative and positive class examples are the same satellite. This was done to ensure that we were isolating our identification problem to features of the electro-optical fiduciary marker and not features of a specific satellite.
5) All Positive and Negative Class Examples Use The Same Sensors: The ground-based and space-based sensors are the same across all datasets.

C. Machine Learning Pipeline

From a machine learning perspective our goal was simply to build models that would enable us to test our idea of identifying a satellite by an electro-optical marker. While we wanted to ensure that our models would generalize and perform well, we were not concerned with producing production quality models at this stage in our research. The machine learning pipeline we implemented to explore our ideas reflects our objectives.

Our machine learning pipeline depicted in Fig. 5, includes the full life cycle of the training and evaluating machine learning models. The training and evaluation of machine learning models is a cyclical process. Below is a brief discussion of pipeline details:

1) Data ingestion & preprocessing: This step includes converting bitmaps to grayscale .png files, flattening image vectors and adding numeric, binary labels to positive (class 1) and negative (class 0) examples for ease of use in analysis etc.

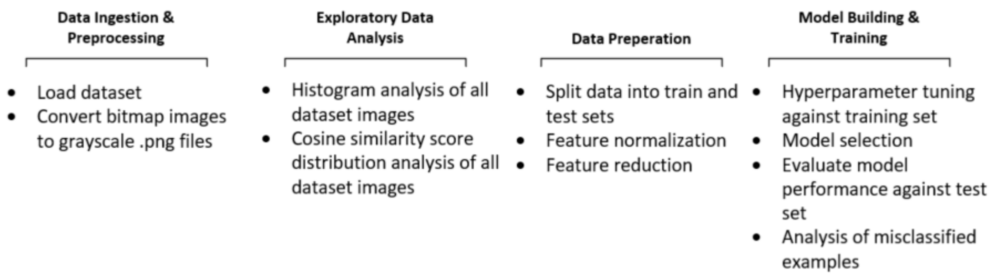

Fig. 5 Machine learning pipeline for data processing, analysis, model training and evaluation.

2) Exploratory data analysis:
    1) Histogram analysis: Analysis to understand the datasets we generated. More specifically it gave us an understanding of how different/similar satellite images with and without electro-optical markers are.
    2) Cosine similarity analysis: Analysis to gain understanding of the cosine similarity score distribution of satellite images with electro-optical markers vs satellite images without electro-optical markers.
3) Data preparation: This step includes doing a standard 80/20, shuffled train/test split on the dataset under analysis, min-max scaling to normalize features (pixel intensity values) and principal component analysis (PCA) based feature reduction.
4) Model building & training: This step includes hyperparameter tuning via k-fold cross validation (CV) against the training set, training a SVM binary classifier with best fit parameters against the training set and evaluating model performance against the test set. Performance analysis includes analysis of misclassified examples.
    1) We used 10-fold CV for shorter duration datasets and 5-fold CV for longer duration datasets. We choose a smaller value of k for longer duration datasets to minimize time complexity of convergence of hyperparameter selection. The smaller value of k for longer duration datasets produced comparable best fit parameters as using 10-fold CV.
    2) Misclassified example analysis was done via histogram analysis and visual image inspection.

We shuffled the data during the train/test split process to mitigate the possible impact of the sequential nature of the datasets on classifier performance and more specifically on a model's ability to generalize. All datasets were generated and initially ingested in ascending order by frame number. Given that from a machine learning perspective, the goal of this preliminary research was to test the efficacy of identifying a satellite with an electro-optical fiduciary marker at any given point in time, shuffling the data was a way remove the possibility of temporal components impacting classifier performance. While formal drift analysis was not conducted it was assumed that the sequential nature of our datasets could negatively impact classifier performance or at the very least produce classifiers that would treat the sequential order of the data as a relevant predictor.

IV. Results and Discussion

The performance noted in Table 4 of our classifier models shows it is possible to accurately identify a satellite that has an electro-optical fiduciary marker using both ground and space-based sensors. Model performance also reflects our objective to model the problem as simply as possible so that we could focus on testing the efficacy of our idea; with the understanding that future research efforts would focus on more complex and nuanced versions of this problem.

A. Marker Visibility, Scenario Duration and Model Performance

From a qualitative perspective, in both the shorter and longer duration experiments the ground and space-based sensors were able to see markers most of the time in the positive examples. By positive examples we mean that the markers were present on the primary panel, but due to the range or perspective from the observing sensor, the markers were out of view or not distinguishable. This directly impacted the ability of our models to accurately predict the satellite with the electro-optical fiduciary marker. Based on our visual inspection of all frames across all four datasets, it was possible to easily distinguish the markers in over 50% of the frames. In fact, as noted in Table 5 for the shorter duration, space-based sensor the marker was visible in almost 100% of the frames.

Table 4 Summary of classifier model performance

SVM Model	Features	Accuracy
Ground Sensor (Short Duration)	Pixel Intensity Values	0.88
Satellite Sensor (Short Duration)	Pixel Intensity Values	0.98
Ground Sensor (Long Duration)	Pixel Intensity Values	0.97
Satellite Sensor (Long Duration)	Pixel Intensity Values	0.90

Table 5 Approximate number of positive example frames where the electro-optical fiduciary marker is visibly distinguishable by dataset.

Dataset	# Of Frames	# Of Frames With A Visible Marker	% Of Frames With A Visible Marker
Ground Sensor (Short Duration)	120	98	82%
Satellite Sensor (Short Duration)	120	119	99%
Ground Sensor (Long Duration)	1580	865	56%
Satellite Sensor (Long Duration)	1580	972	62%

The relationship between marker visibility and scenario duration had an impact on overall model performance. This relationship was apparent during our preliminary experiments using shorter duration datasets. While we did get meaningful results, the near perfect performance of the shorter duration, space-based model as shown in Fig. 6 led us to generate longer duration datasets to confirm that our models weren't simply memorizing images or overfitting due to smaller dataset size. We wanted to confirm that our models were generalizing on the problem as modeled in our generated datasets.

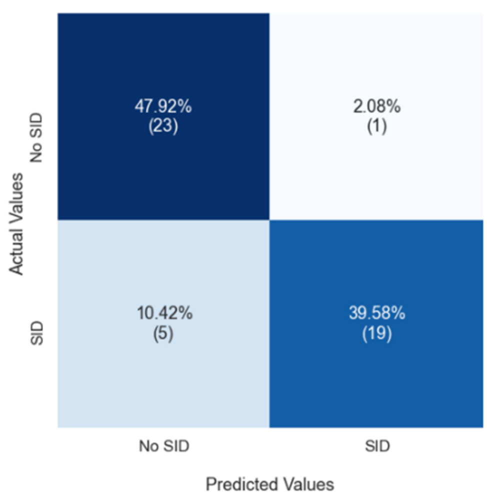

(a)

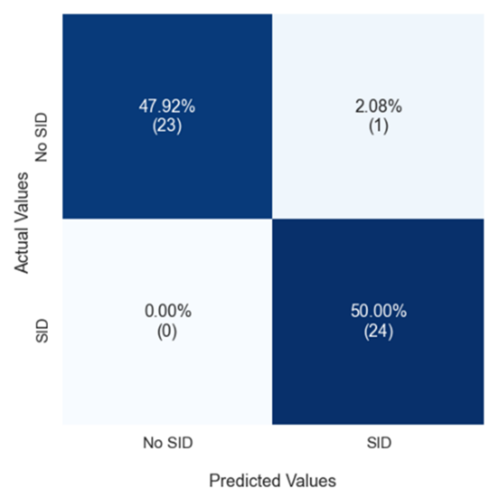

(b)

Fig. 6 Shorter duration classifier model performance: (a) shorter duration ground sensor model confusion matrix, (b) shorter duration space sensor model confusion matrix.

The performance of the longer duration models as depicted in Fig. 7 confirmed the efficacy of our idea to identify a satellite that has an electro-optical fiduciary marker using both ground and space-based sensors. The results also confirmed the following:

1) Pixel intensity values of gray scale images contained enough information to accurately identify a satellite that

has an electro-optical fiduciary marker using both ground and space-based sensors.
2) The performance of the shorter duration models were accurate and reflected the high percentage of frames where the ground and space-based sensors could see the markers.
3) All models struggled to accurately predict the satellite with the marker once the marker was out of the sensor's boresight in the positive examples. This was true for both ground and space-based sensors. These blind spots introduced an ambiguity between positive and negative examples. This ambiguity is reflected in all misclassified examples, across all experiments.

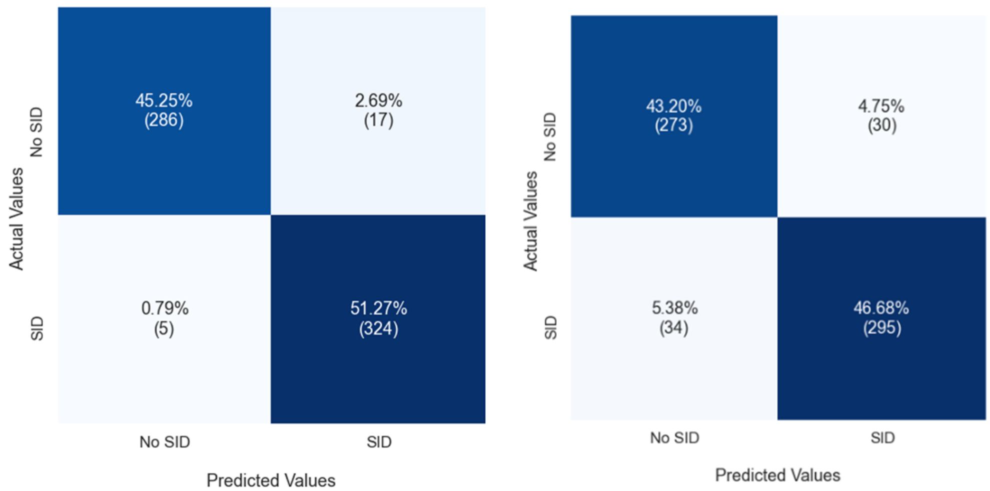

(a) **(b)**

Fig. 7 Longer duration classifier model performance: (a) longer duration ground sensor model confusion matrix, (b) longer duration space sensor model confusion matrix.

B. Misclassified Examples Analysis

The analysis of all misclassified examples across all experiments confirmed that the ambiguity introduced when the electro-optical fiduciary marker was no longer visible to the sensor's boresight caused our classifier models to struggle to make accurate predictions. This phenomenon also confirmed our hypothesis that electro-optical fiduciary markers placed on only a single side of a satellite could confuse ground and space-based sensors. Lastly, these results highlight a known weakness in traditional SVM models where prediction accuracy can be negatively impacted by overlapping examples [17]. In all datasets, feature overlap is introduced via positive class examples where the marker is out of the sensor's boresight. Approaches to address overlapping examples will be explored in subsequent research. Fig. 8 shows examples of misclassification of overlapping test sets.

Further analysis is required to better understand the relation between scenario duration, attitude, and sensor location with respect to satellite detection tasks using electro-optical fiduciary markers. This analysis is slated for future work.

V. Improvements and Future Work

While our preliminary results are promising, we plan to generate and test with more nuanced and complex datasets. By generating datasets with a larger number of examples, variations in noise, sensor models, satellite models, attitudes, wavebands, class distribution and multiple classes, we will be able to further demonstrate the strengths and weaknesses of our approach as well as the novel contributions of our research. In addition to improving the size and robustness of our datasets, we are exploring using different sets of image features as well as evaluating the performance of different machine learning models.

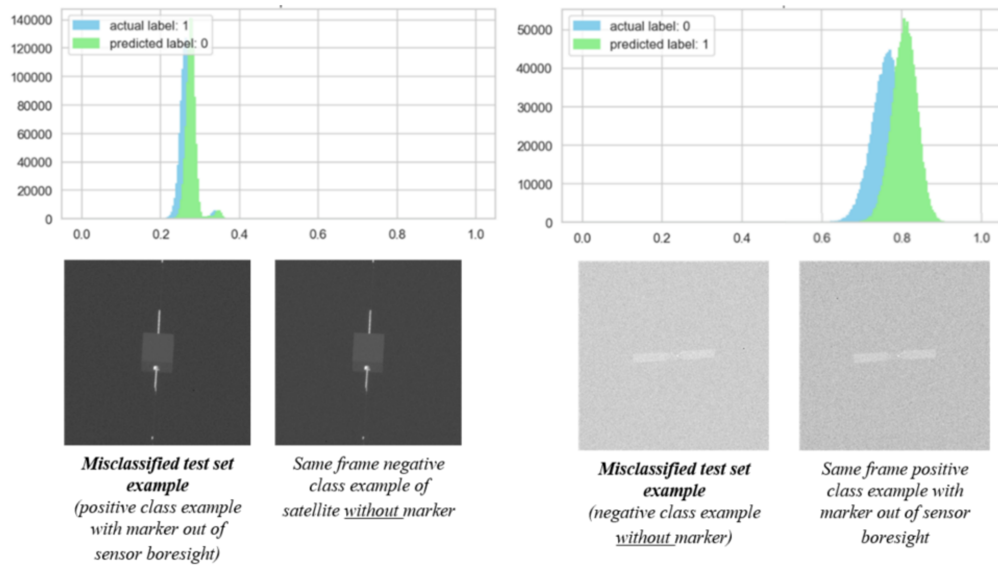

(a) (b)

Fig. 8 Test set misclassified examples: (a) histogram comparing misclassified positive example with its corresponding frame's negative example (b) histogram comparing misclassified negative example with its corresponding frame's positive example.

VI. Conclusion

This work contained a twofold challenge. To explore the application of electro-optical fiducial markers for identification. Additionally, we explored how to prove this novel solution with synthetic data and machine learning.

Beginning with simulated data, generated by STK, and combining it with a machine learning classifier, we see this workflow as a successful method for addressing the challenges of identifying RSOs. The results of this study also demonstrate how fiducial markers on the body of a satellite can be used to identify an object. By designing a balanced dataset of images of a satellite with and without fiducial markers, we were able to focus this study and understand the causes of misclassifications. We learned that a potential solution to misclassifications would be to place additional markers on all sides of the satellite so a sensor from any perspective would be able to view them.

By having a unique spectral signature, distinguishing it from other RSOs, it has been demonstrated that an exploitation algorithm can identify one satellite from another. Therefore, we propose electro-optical fiducial markers on satellites as a method of identification and synthetic data with machine learning to evaluate them.

Acknowledgments

We would like to thank Ansys Government Initiatives (AGI) for the use of Systems Tool Kit (STK) which allowed us to generate the data used in this analysis. Additional thanks to Randall Scott Cross, Senior Technical Support Engineer, for creating a custom 3D satellite model that we could use in this work.

References

[1] Pyrak, M., and Anderson, J., "Performance of Northrop Grumman's Mission Extension Vehicle (MEV) RPO imagers at GEO," *Autonomous Systems: Sensors, Processing and Security for Ground, Air, Sea and Space Vehicles and Infrastructure 2022*, Vol. 12115, SPIE, 2022, pp. 64–82.

[2] Anderson, R., and Cantwell, G., "EOIR Model Description and Validation," help.agi.com, 2010. URL `https://help.agi.com/stk/LinkedDocuments/EOIRModelDescriptionandValidation.pdf`, [retrieved 01 March 2022].

[3] Christianini, N., and Shawe-Taylor, J., "An Introduction to Support Vector Machines. Cambridge University Press," , 2000.

[4] Vapnik, V. N., "Statistical learning theory," *Adaptive and learning systems for signal processing communications and control*, 1998.

[5] McQuaid, I. W., "Autonomous association of geo RSO observations using deep neural networks," Tech. rep., Air Force Institute of Technology Wright-Patterson AFB OH Wright-Patterson AFB, 2018.

[6] Fukushima, K., "Neocognitron: A self-organizing neural network model for a mechanism of pattern recognition unaffected by shift in position," *Biological Cybernetics*, Vol. 36, 1980, p. 193–202.

[7] Lecun, Y., Bottou, L., Bengio, Y., and Haffner, P., "Gradient-based learning applied to document recognition," *Proceedings of the IEEE*, Vol. 86, No. 11, 1998, pp. 2278–2324.

[8] Fletcher, J., McQuaid, I., Thomas, P., Sanders, J., and Martin, G., "Feature-based satellite detection using convolutional neural networks," *Proceedings of the Advanced Maui Optical and Space Surveillance Technologies Conference*, 2019, p. 11.

[9] Gazak, J. Z., McQuaid, I., Swindle, R., Phelps, M., and Fletcher, J., "SpectraNet: Learned Recognition of Artificial Satellites from High Contrast Spectroscopic Imagery," *Proceedings of the IEEE/CVF Winter Conference on Applications of Computer Vision*, 2022, pp. 4012–4020.

[10] Perez, M., Mohamed Ali, M. A., Garcia Sanchez, A., Ghorbel, E., Al Ismaeil, K., Le Henaff, P., and Aouada, D., "Detection & Identification of On-Orbit Objects Using Machine Learning," *European Conference on Space Debris*, Vol. 8, 2021.

[11] Dhivya, P., and Vasuki, S., "Wavelet based MRI brain image classification using radial basis function in SVM," *2018 2nd International Conference on Trends in Electronics and Informatics (ICOEI)*, 2018, pp. 1–9.

[12] Castro, W., Oblitas, J., De-La-Torre, M., Cotrina, C., Bazán, K., and Avila-George, H., "Classification of cape gooseberry fruit according to its level of ripeness using machine learning techniques and different color spaces," *IEEE access*, Vol. 7, 2019, pp. 27389–27400.

[13] Wang, C., Bai, Y., López-Sanjuan, C., Yuan, H., Wang, S., Liu, J., Sobral, D., Baqui, P., Martín, E., Galarza, C. A., et al., "J-PLUS: Support vector machine applied to STAR-GALAXY-QSO classification," *Astronomy & Astrophysics*, Vol. 659, 2022, p. A144.

[14] Manning, C. D., Raghavan, P., and Hinrich, S., Cambridge University Press, 2008, p. 293–320.

[15] STK, Systems Tool Kit, Software Package, Ver 12.4, Ansys Government Initiatives (AGI), Exton, PA, 2022.

[16] Henninger, J. H., *Solar absorptance and thermal emittance of some common spacecraft thermal-control coatings*, Vol. 1121, National Aeronautics and Space Administration, Scientific and Technical Information Branch, 1984.

[17] Tang, Y., and Gao, J., "Improved Classification for Problem Involving Overlapping Patterns," *TRANSACTIONS on Information and Systems 90.11*, Vol. E90-D, No. 11, 2007, p. 1787–1795.